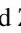




Electro-optical properties of excitons in Cu₂O quantum wells. II. Continuum statesDavid Ziemkiewicz ^{*}, Gerard Czajkowski, Karol Karpiński , and Sylwia Zielińska-Raczyńska *Institute of Mathematics and Physics, UTP University of Science and Technology, Aleje Prof. S. Kaliskiego 7, 85-789 Bydgoszcz, Poland*

(Received 27 April 2021; revised 26 July 2021; accepted 16 August 2021; published 25 August 2021)

We present a theoretical calculation of optical functions for a Cu₂O quantum well (QW) with Rydberg excitons. In particular, an external homogeneous electric field parallel to the QW plane is considered and the spectra are obtained in the energy region above the effective band gap, which is a suitable condition to observe the Franz-Keldysh (FK) oscillations. We quantitatively describe the amplitudes and periodicity of FK modulations and the influence of both Rydberg excitons and confinement effect on this phenomenon.

DOI: [10.1103/PhysRevB.104.075304](https://doi.org/10.1103/PhysRevB.104.075304)**I. INTRODUCTION**

In recent years, there has been much interest in the optical properties of Rydberg excitons (REs) in bulk semiconductors in the context of their unusual capabilities while interacting with external fields [1,2], with particular applications in quantum information processing [3,4]. Later, the studies were extended to the electro-optic properties of bulk Cu₂O crystals in the energy region above the fundamental gap, where the oscillations appear [5]; this is often referred to as the Franz-Keldysh effect [6,7].

An externally applied electric field affects the absorption edge via the Franz-Keldysh effect, which is the result of wave functions “leaking” into the band gap. Due to the electric field, the electron and hole wave functions become Airy functions, which are characterized by a “tail” extending into the classically forbidden band gap. The absorption spectrum is modified: a tail at energies below the band gap and some oscillations above it are observed.

This phenomenon was considered before in low-dimensional structures such as quantum wires, nanobelts [8–10], and carbon nanotubes [11]. Miller *et al.* [12], Trallero [13], and Merbach *et al.* [14] studied the confined Franz-Keldysh effect in quantum wells with an electric field along the direction of carrier confinement. Xia and Spector [10,15] presented theoretical studies of the Franz-Keldysh (FK) effect in the interband optical absorption for various nanostructures: quantum wires, wires, and boxes. However, the excitonic effects were neglected in these papers.

The topic of the FK effect in low-dimensional nanostructures, particularly with REs, has not been covered yet. In our previous work [16], we studied quantum wells with Rydberg excitons situated in an external electric field below the transition energy. In this work, we concentrate on the case in which an electric field is parallel to the direction of the quantum well plane, for the excitation energies region above the effective band gap; the external field influences the continuum states. In such a situation, the Franz-Keldysh

oscillations appear, analogous to the bulk case, but modified due to the reduced dimensionality. However, in the quantum well, the physical picture becomes more complicated because there is an interplay between the strong Coulomb interaction of particles forming the exciton, a constraint superimposed by confinement and continuum. Moreover, the effect of excitons may influence the optical properties near the band gap [17], so the situation might become more complex when one considers conditions superimposed by quantum wells’ potential barriers [11]. Even though the excitonic impact is not very important for the position of resonances, it is significant for the magnitude of the absorption.

Cuprous oxide is a material where Rydberg excitons in quantum wells can be created [18]. In the future, it can be possible to fabricate low-dimensional structures, which can provide capabilities to create scalable quantum devices. Taking advantage of above-the-gap oscillations typical of the Franz-Keldysh effect might pave the way to design the flexible electromodulators. The theoretical description of the FK effect in Cu₂O quantum wells (QWs) with REs requires the continuum states to be taken into account. With the help of the real density matrix approach, we will derive analytical formulas for the periodically modulated electro-optical susceptibility for QWs, both without and with Rydberg excitons.

The paper is organized as follows. In Sec. II, we will present the formal theory of electroabsorption in a quantum well for the energy region above the effective gap, which differs from the fundamental gap due to the confinement character of the system. Section III contains the presentation of illustrative results of the Franz-Keldysh oscillations, and discusses the effects of multiple confinement states arising from a limited QW thickness and the effect of excitonic states on the spectrum above the effective gap. Finally, in Sec. IV, general conclusions are presented.

II. THEORY

We consider the case of quantum wells when the external electric field is parallel to the QW planes (a lateral electric field) and it is perpendicular to the direction of the confinement; our aim is to describe its optical response in the situation

^{*}david.ziemkiewicz@utp.edu.pl

in which the electromagnetic wave propagates in the z direction and excites states above the effective gap E'_g . As described in our first paper [16], a Cu_2O quantum well of thickness L , located in the xy plane, with QW surfaces located at $z = \pm L/2$ is considered. A linearly polarized electromagnetic wave of frequency ω and the electric vector \mathbf{E} incident normally on the QW ($\vec{k} \parallel z$) is considered.

The problem will be examined using the real density matrix approach (RDMA), as done in our preceding paper [16].

It should be noted that the proper estimation of effective masses allows for inclusion of the influence of admixture of the lower valence subband [19]. By using effective masses experimentally measured in similar, confined systems, these effects are implicitly included [16].

There, the scheme which enables one to calculate the electro-optical functions for a cuprous oxide QW with REs has been described for the case of excitation energy smaller than E'_g , with a step-by-step derivation. Here we consider the excitation energy above the transition energy, invoking only the main points of the derivation. The optical functions will be obtained by solving a system of integro-differential equations, consisting of the so-called constitutive equation $(H_{QW} - \hbar\omega - i\Gamma)Y = \mathbf{M}\mathbf{E}$ together with the Maxwell equation [5]. The coefficient Γ represents the dissipative processes. In the case in which the external electric field \mathbf{F} is parallel to the Ox axis, the constitutive equation has the form

$$\partial_t Y + \frac{i}{\hbar} \left[E_g - \frac{\hbar^2}{2m_e} \partial_{z_e}^2 - \frac{\hbar^2}{2m_h} \partial_{z_h}^2 - \frac{\hbar^2}{2\mu} \partial_x^2 - \frac{\hbar^2}{2\mu} \partial_y^2 + eFx + V_{eh}(x, y) + V_{\text{conf}}(z_e, z_h) - i\Gamma \right] Y = \frac{i}{\hbar} \mathbf{M}\mathbf{E}, \quad (1)$$

where \mathbf{M} is the smeared-out transition dipole density and Y is the bilocal coherent electron-hole (e-h) amplitude. The confinement potential V_{conf} is taken in the parabolic form,

$$V_{\text{conf}} = \frac{1}{2} m_e \omega_{ez}^2 z_e^2 + \frac{1}{2} m_h \omega_{hz}^2 z_h^2, \quad (2)$$

and the e-h interaction potential in the two-dimensional form is $V_{eh} = -\frac{e^2}{4\pi\epsilon_0\epsilon_b\rho}$ with the relative coordinate ρ . Since we consider rather shallow QWs, the strong confinement limit is used. The weak confinement, which corresponds to the exciton center-of-mass quantization, is appropriate for larger nanocrystals (see, for example, [18]) or bulk crystals [20]. Overall, since the spatial extension of the exciton is proportional to the square of exciton number j^2 , for higher states it very quickly becomes much larger than the well thickness L , justifying the two-dimensional approximation. The above equation will be solved by the method elaborately described in Ref. [5]. We separate the Hamiltonian of Eq. (1) into the “kinetic+electric field” part $H_{\text{kin}+F}$ and the electron-hole interaction term V , to obtain

$$H_{\text{kin}+F} Y = M E_x - V Y, \quad (3)$$

where E_x is the x component of the electric vector \mathbf{E} . The above relation is a Lippmann-Schwinger equation [5], which can be solved by the means of the Green's function G ,

$$Y = G M E_x - G V Y. \quad (4)$$

TABLE I. Band parameter values for Cu_2O , Rydberg energy, and excitonic radius calculated from effective masses; masses in free electron mass m_0 .

Parameter	Value	Unit	Reference
E_g	2172.08	meV	[22]
R^*	87.78	meV	[22]
Δ_{LT}	1.25×10^{-3}	meV	[22]
Γ	$3.88/(j+1)^3$	meV	[23]
m_e	1.0	m_0	[22]
m_h	0.7	m_0	[22]
M_{tot}	1.56	m_0	[22]
μ	0.363	m_0	[22]
a^*	1.1	nm	[22]
r_0	0.22	nm	[22]
ϵ_b	7.5		[22]
F_1	1.02×10^3	kV/cm	

Considering the electron and hole confinement states N_e, N_h , the Green function will have the form

$$G = \sum_{N_e, N_h} \psi_{\alpha_e, N_e}^{(1D)}(z_e) \psi_{\alpha_e, N_e}^{(1D)}(z'_e) \psi_{\alpha_h, N_h}^{(1D)}(z_h) \psi_{\alpha_h, N_h}^{(1D)}(z'_h) \times \frac{2}{\pi} \int_0^\infty dq \sin qy' \sin qy g_{N_e, N_h, q}(x, x'), \quad (5)$$

with

$$g_{N_e, N_h, q}(x, x') = g_{N_e, N_h}^< g_{N_e, N_h}^>, \\ g_{N_e, N_h, q}^< = \frac{\pi}{f^{1/3}} \text{Bi} \left[f^{1/3} \left(x^< + \frac{\kappa_{N_e, N_h}^2 + q^2}{f} \right) \right] + i \text{Ai} \left[f^{1/3} \left(x^< + \frac{\kappa_{N_e, N_h}^2 + q^2}{f} \right) \right], \\ g^> = \text{Ai} \left[f^{1/3} \left(x^> + \frac{\kappa_{N_e, N_h}^2 + q^2}{f} \right) \right], \quad (6)$$

where $x^< = \min(x, x')$ and $x^> = \max(x, x')$, $\text{Ai}(x)$ and $\text{Bi}(x)$ are the Airy functions (see, for example, Ref. [21]), and

$$\kappa_{N_e, N_h}^2 = \frac{2\mu}{\hbar^2} a^{*2} (E_g + W_{N_e} + W_{N_h} - \hbar\omega - i\Gamma_{N_e, N_h}). \quad (7)$$

W_{N_e} and W_{N_h} are the confinement energies of the electron and the hole. We introduce the parameter f , which defines the relative electric field strength and the ionization field,

$$f = \frac{F}{F_1}, \quad F_1 = \frac{\hbar^2}{2\mu e a^{*3}} = \frac{R^*}{a^* e}, \quad (8)$$

with excitonic Rydberg R^* and corresponding excitonic Bohr radius a^* . The full set of the used parameters is shown in Table I. The confinement functions $\psi_{N_e}^{(1D)}(z_e)$, $\psi_{N_h}^{(1D)}(z_h)$ are the quantum oscillator eigenfunctions of the form

$$\psi_{\alpha, N}^{(1D)}(z) = \pi^{-1/4} \sqrt{\frac{\alpha}{2^N N!}} H_N(\alpha z) e^{-\frac{\alpha^2}{2} z^2}, \\ \alpha = \sqrt{\frac{m\omega_z}{\hbar}}, \quad (9)$$

where $H_N(x)$ are Hermite polynomials ($N = 0, 1, \dots$). The dipole density M is given by the formula

$$M = \frac{M_0}{\rho_0^2} \delta(x) y e^{-\frac{x^2}{2\rho_0^2}} \delta(z_e - z_h). \quad (10)$$

The Lippmann-Schwinger equation (3) is an integral equation, which can be solved in several ways. We choose the method of a one-parameter probe function and present in detail the way of conducting these intricate calculations. To confirm the correctness of our results, we will independently use two alternative approximations with two expressions for the probe functions and with two forms for the electron-hole attraction potential. Here we note that for excitation energies above the gap and with the applied electric field, the carriers move freely and the attraction potential has a small impact on the optical properties. Thus, as will be shown later, both approaches provide very similar results.

In the first approximation, the probe function has the form

$$Y = Y_0 y e^{-\kappa_{00} \sqrt{x^2+y^2}} \psi_{\alpha_e,0}^{(1D)}(z_e) \psi_{\alpha_h,0}^{(1D)}(z_h), \quad (11)$$

with κ_{00} given by Eq. (7) and unknown parameter Y_0 , which will be obtained from Eq. (4). The function Y is then inserted into the expression for the total polarization of the medium, $P(Z) = 2\text{Re} \int dx dy \mathbf{M}(x, y) Y(x, y, Z)$, where Z is the center-of-mass coordinate. Using the long-wave approximation, we obtain the mean effective susceptibility,

$$\chi = \frac{1}{L} \int_{-L/2}^{L/2} \frac{P(Z)}{\epsilon_0 E(Z)} dZ, \quad (12)$$

which, basing on Eqs. (5) and (10), can be written in the form

$$\begin{aligned} \chi &= \frac{2}{\epsilon_0} \int_{-L/2}^{L/2} \frac{1}{Q} M^* G M dZ \\ &= \frac{8}{3f^{1/3}} \frac{\epsilon_b \Delta_{LT}}{R^*} e^{4\rho_0} \left(\frac{a^*}{L} \right) \\ &\quad \times \sum_{N=0}^{N_{\max}} \langle \Psi_{NN} \rangle_L \frac{1}{Q} \int_0^\infty dq q^2 e^{-\rho_0^2 q^2} \times \left[\text{Bi} \left(\frac{\kappa_{NN}^2 + q^2}{f^{2/3}} \right) \right. \\ &\quad \left. \times \text{Ai} \left(\frac{\kappa_{NN}^2 + q^2}{f^{2/3}} \right) + i \text{Ai}^2 \left(\frac{\kappa_{NN}^2 + q^2}{f^{2/3}} \right) \right]. \quad (13) \end{aligned}$$

The resonant denominator Q is defined as

$$\begin{aligned} Q &= 1 - \frac{MGVY}{MY} \\ &= 1 - \left[\exp \left(\frac{\kappa_{00}^2 \rho_0^2}{4} \right) D_{-3}(\kappa_{00} \rho_0) \right]^{-1} \frac{\sqrt{2\pi}}{f^{1/3}} \\ &\quad \times \left\{ \int_0^\infty dq \frac{q^2}{\sqrt{q^2 + \kappa_{00}^2}} e^{-q^2 \rho_0^2/2} \text{Ai} \left(\frac{\kappa_{N_e N_h}^2 + q^2}{f^{2/3}} \right) \right. \\ &\quad \times \int_0^\infty dx x K_1 \left(x \sqrt{q^2 + \kappa_{00}^2} \right) \left[\text{Bi} \left(\frac{\kappa_{N_e N_h}^2 + q^2}{f^{2/3}} - f^{1/3} x \right) \right. \\ &\quad \left. \left. + i \text{Ai} \left(\frac{\kappa_{N_e N_h}^2 + q^2}{f^{2/3}} - f^{1/3} x \right) \right] \right\} \end{aligned}$$

$$\begin{aligned} &+ \int_0^\infty dq \frac{q^2}{\sqrt{q^2 + \kappa_{00}^2}} e^{-q^2 \rho_0^2/2} \left[\text{Bi} \left(\frac{\kappa_{N_e N_h}^2 + q^2}{f^{2/3}} \right) \right. \\ &+ i \text{Ai} \left(\frac{\kappa_{N_e N_h}^2 + q^2}{f^{2/3}} \right) \left. \right] \\ &\times \int_0^\infty dx x K_1 \left(x \sqrt{q^2 + \kappa_{00}^2} \right) \text{Ai} \left(\frac{\kappa_{N_e N_h}^2 + q^2}{f^{2/3}} + f^{1/3} x \right) \Bigg\}, \quad (14) \end{aligned}$$

where $D_\nu(z)$ is the parabolic cylinder function [21], and $K_1(z)$ is the modified Bessel function of the second kind.

Regarding the properties of Airy functions, it is known that for a negative argument, they show oscillatory behavior. As follows from Eq. (13), the absorption, being the imaginary part of the susceptibility, will show oscillations known as Franz-Keldysh oscillations (Franz-Keldysh effect). Considering the quantum well geometry, this effect is also termed the two-dimensional FK effect (or, alternatively, lateral FK effect).

To point out the differences between two- and three-dimensional structures, we can compare the absorption of quantum well and bulk systems [5]. As the first approximation, one can omit the resonant denominator Q ; by examining Eq. (14), one can see that $Q \approx 1$ is a particularly good approximation in the limit of large f or energy far above E_g , which results in large κ_{00}^2 in the first exponential function of Eq. (14). With such assumption, for the two-dimensional system, one obtains

$$\begin{aligned} \text{Im} \chi^{2D} &= \chi' \left(\frac{a^*}{L} \right) \sum_{N=0}^{N_{\max}} \langle \Psi_{NN} \rangle_L \exp(-\mathcal{E}_N f^{2/3}) f^{2/3} \\ &\quad \times \int_{-\mathcal{E}_N}^\infty du (u + \mathcal{E}_N)^{1/2} e^{-\rho_0^2 f^{2/3} u} \text{Ai}^2(u), \\ \mathcal{E}_N &= \lim_{\Gamma \rightarrow 0} \frac{\hbar\omega - E_g - W_{N_e} - W_{N_h} + i\Gamma}{\hbar\Theta}, \\ N_e = N_h = N, \quad \hbar\Theta &= R^* f^{2/3}, \\ \chi' &= \frac{4}{3} \frac{\epsilon_b \Delta_{LT}}{R^*} e^{4\rho_0}, \quad (15) \end{aligned}$$

while for the bulk case, the susceptibility was described by the following formula [5]:

$$\begin{aligned} \text{Im} \chi^{3D} &= \chi' \exp(-\mathcal{E} f^{2/3}) f \\ &\quad \times \int_{-\mathcal{E}}^\infty du (u + \mathcal{E}) e^{-\rho_0^2 f^{2/3} u} \text{Ai}^2(u), \\ \mathcal{E} &= \lim_{\Gamma \rightarrow 0} \frac{\hbar\omega - E_g + i\Gamma}{\hbar\Theta}. \quad (16) \end{aligned}$$

The maxima of oscillations for the QW are estimated as

$$E_{Nn} = E_g + W_{ne} + W_{nh} + \left(\frac{3}{3} n_{fk} \pi \right)^{2/3} \hbar\theta, \quad (17)$$

where n_{fk} is the number of the maximum. They are similar to those in the bulk case [5], but are modified by the addition of the constant energy shift, $W_{ne} + W_{nh}$. The precise calculation of the resonant term Q given by Eq. (14) can be

numerically challenging due to the multiple integrals containing Airy functions, which exhibit an oscillatory behavior and cannot be easily truncated to finite integration limits. Moreover, their arguments diverge for $f \rightarrow 0$, which leads to an infinite value of B_i and indefinite value of A_i . Thus, a more robust approach may be needed for some cases. One can take advantage of the fact that the excitons provide only a small correction to the FK spectrum, which is relatively insensitive to the form of the Coulomb potential. Therefore, one of the options to simplify the numerical calculations and increase

their robustness is to use a different electron-hole potential of the form

$$V(x, y) = V_0 e^{-v^2 y^2} \delta(x), \quad (18)$$

with the corresponding probe function Y ,

$$Y = Y_0 y \exp[-|\kappa_{00}^2|(x^2 + y^2)] \Psi_{00}(z_e, z_h). \quad (19)$$

The parameters V_0, v are chosen to fit the position of the lowest excitonic resonance. After substituting them into Eq. (14), one gets

$$\begin{aligned} \frac{MGVY}{MY} &= V_0 \left\{ \frac{1 + 2|\kappa_{00}^2|\rho_0^2}{2(|\kappa_{00}^2| + v^2)} \right\}^{3/2} \sqrt{\frac{\pi}{2}} f^{1/3} \left\{ \int_0^{\mathcal{E}_0} e^{-sf^{2/3}(\mathcal{E}_0 - u)} \sqrt{\mathcal{E}_0 - u} [\text{Bi}(-u) + i\text{Ai}(-u)] \text{Ai}(-u) du \right. \\ &\quad \left. + \int_0^\infty e^{-sf^{2/3}(\mathcal{E}_0 + u)} \sqrt{u + \mathcal{E}_0} [\text{Bi}(u) + i\text{Ai}(u)] \text{Ai}(u) du \right\}, \\ s &= \frac{\rho_0^2}{2} + \frac{1}{4(|\kappa_{00}^2| + v^2)}, \\ \mathcal{E}_0 &= -\frac{\kappa_{00}^2}{f^{2/3}}, \end{aligned} \quad (20)$$

and, in the limit of $f \rightarrow 0$,

$$\begin{aligned} MGVY_{f \rightarrow 0} &\approx (M_0 \rho_0) Y_0 V_0 \frac{\sqrt{2\pi}}{4\kappa_{00}} \left[\frac{(|\kappa_{00}^2| + v^2)}{2(|\kappa_{00}^2| + v^2)\rho_0^2 + 1} \right]^{3/2}, \\ \frac{MGVY}{MY} &= \frac{(M_0 \rho_0) Y_0 V_0 \frac{\sqrt{2\pi}}{4\kappa_{00}} \left[\frac{(|\kappa_{00}^2| + v^2)}{2(|\kappa_{00}^2| + v^2)\rho_0^2 + 1} \right]^{3/2}}{(M_0 \rho_0) Y_0 \frac{\sqrt{2\pi}}{2} (1 + 2|\kappa_{00}^2|\rho_0^2)^{-3/2}} \\ &= \frac{V_0}{2\kappa_{00}} \left[\frac{(|\kappa_{00}^2| + v^2)(1 + 2|\kappa_{00}^2|\rho_0^2)}{1 + 2(|\kappa_{00}^2| + v^2)\rho_0^2} \right]^{3/2}. \end{aligned}$$

Finally, one arrives at a much simplified expression for Q ,

$$Q = 1 - \frac{MGVY}{MY} = 1 - \frac{V_0}{2\kappa_{00}} \left[\frac{(|\kappa_{00}^2| + v^2)(1 + 2|\kappa_{00}^2|\rho_0^2)}{1 + 2(|\kappa_{00}^2| + v^2)\rho_0^2} \right]^{3/2}, \quad (21)$$

which is then used in Eq. (13). As opposed to Eq. (14), the above relation is not divergent for $f \rightarrow 0$, which makes it a better option for the low field regime. Furthermore, the general influence of the excitons on the spectrum is easier to deduce from Eq. (21); in general, the denominator is slightly smaller than unity, e.g., $Q \sim 1 - \Delta Q$, with $\Delta Q \sim \kappa_{00}^2 \sim \hbar\omega$. Therefore, the inclusion of Q slightly increases the value of susceptibility, with the difference from the no exciton spectrum increasing with energy.

III. RESULTS

We have performed calculations for a Cu_2O quantum well of thickness $L = 10$ nm, in the energetic region above the fundamental band gap. Figure 1 presents the imaginary part of susceptibility calculated from Eq. (15) in the region above the band gap; similarly to the bulk case [5], the Franz-Keldysh oscillations occur. Due to the low amplitudes of these oscillations and a strong increase of overall absorption above

the band gap, the first derivative of susceptibility is shown for better visibility. In Fig. 1(a), one can see the oscillations of the absorption induced by various values of electric field f . The positions of the first four maxima are marked with black lines. One can see that the period of these oscillations decreases with f and it is consistent with the results obtained for the bulk case [5]. However, as compared to the bulk medium, the oscillation amplitude decreases with increasing f . In particular, the initial increase of absorption is much steeper for low f , similar to the results obtained in [11]. The maxima are not evenly spaced; their energy is $E_{\text{max}} \sim n_{fk}^{2/3}$, where n_{fk} is the number of the corresponding maximum [Eq. (17)]. Figure 1(b) shows the dependence of the FK effect on the thickness L . One can observe an energy shift of the order of $\Delta E \sim 50$ meV for $L = 5$ nm that is inversely proportional to L . The oscillation period is unaffected by L . In Fig. 1(c), additional confinement state $N_e = N_h = 1$ is included. The two black spectra at the bottom correspond to $N_e = 0$ and $N_e = 1$; the higher confinement is shifted by ~ 20 meV and both exhibit almost identical

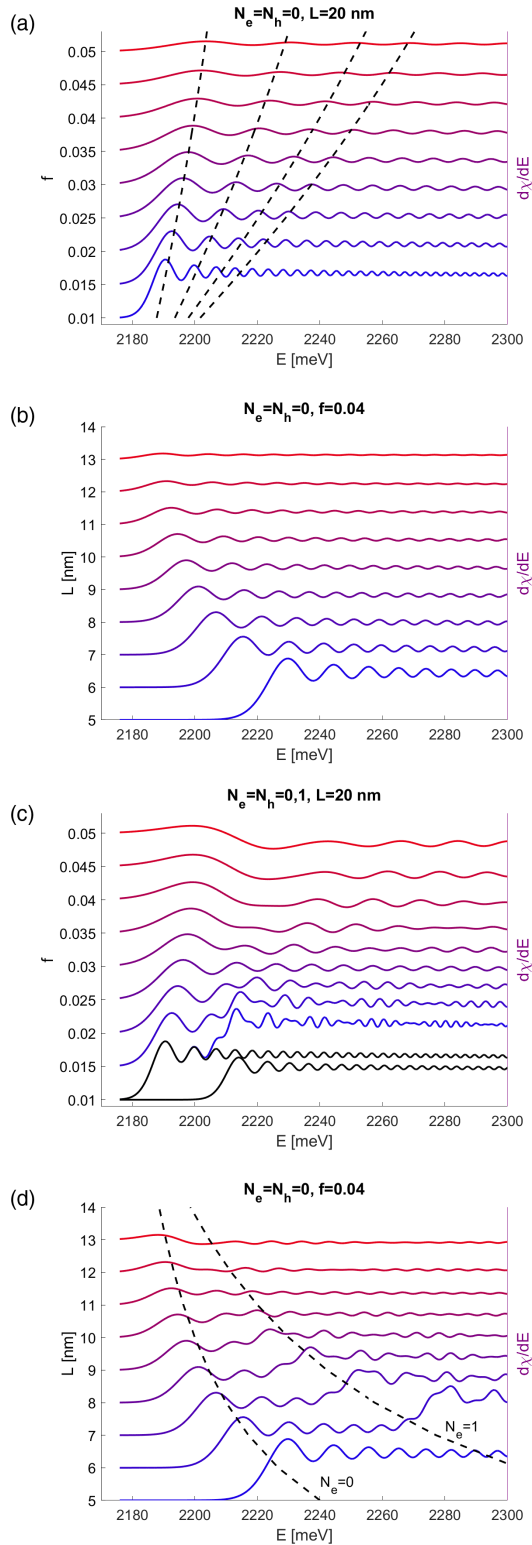


FIG. 1. Imaginary part of susceptibility in the energetic region above the band gap, calculated from Eq. (15) for $L = 10$ nm, $j = 0.9$ and (a) the first confinement state and changing field f (dashed lines mark the first four maxima of absorption), (b) changing thickness L , (c) sum of two lowest confinement states (black lines are spectra for $N_e = N_h = 0$ and $N_e = N_h = 1$, blue line is the sum), (d) two lowest confinement states as a function of thickness.

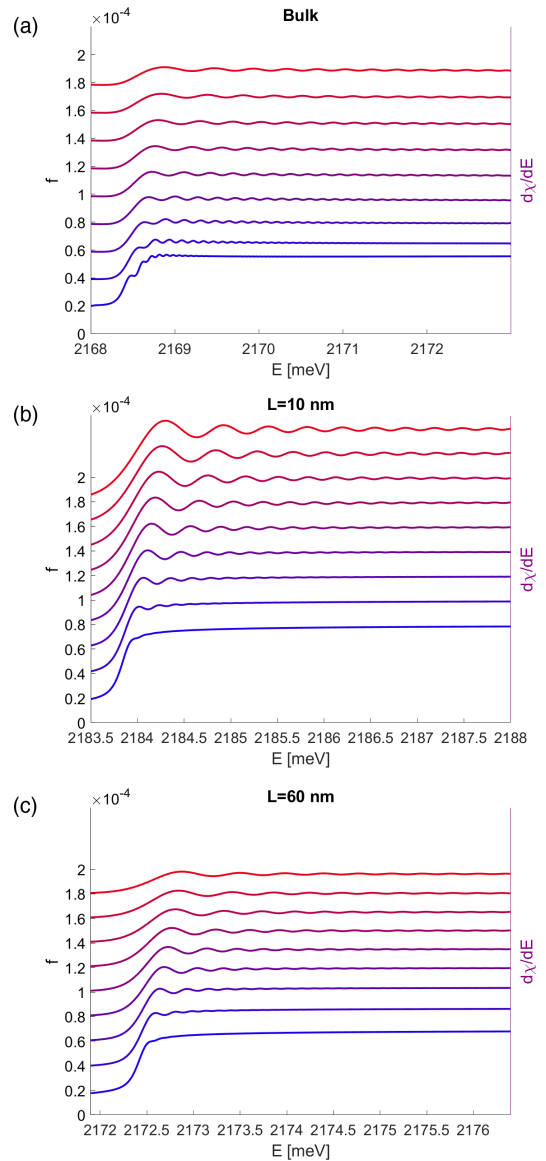


FIG. 2. Imaginary part of susceptibility in the energetic region above the band gap, with comparison of (a) the bulk results and (b) the 10 nm and (c) 60 nm well.

oscillations. Their sum creates a characteristic interference pattern, with a slow sinelike modulation caused by a small difference of the frequencies, similar to the results presented in [10]. Finally, in Fig. 1(d), one can observe that the higher confinement state reacts more strongly to the reduction of the thickness L . This means that the effect of higher confinement states is only noticeable for $L < 10$ nm. On the other hand, the energy of these higher states quickly diverges for low L . As a result, only the two lowest states [marked with black lines in Fig. 1(d)] fit in the considered energy range. In general, the system is capable of producing complicated interference patterns in the high energy part of the spectrum $E \gg E_g$, with two degrees of freedom (L and f) available for tuning them.

To stress the difference between the FK effect in the bulk and QW, Fig. 2 shows a comparison of the calculation results with the bulk spectra obtained in [5]. Again, the first

derivative of susceptibility is shown for clarity. For the case of a low well thickness [Fig. 2(b)], one can notice several differences when compared with bulk results [Fig. 2(a)]. In the quantum well, there is an increase of the absorption slope ($\partial\chi/\partial E$) for energy below the first maximum of oscillation, which is less pronounced in the bulk results. Moreover, the oscillations vanish for very small values of f due to the fact that in the limit of $f = 0$, the susceptibility becomes a slowly increasing function of $(E - E_g)$. For stronger fields, the oscillations are more pronounced than in the bulk case. Due to the fact that $f \ll 1$, $f^{2/3} > f^1$ and the expression for the susceptibility in a confined system in Eq. (15) has an amplitude that is overall higher and decreases more slowly with f . Notably, the period of oscillations is the same in the bulk and QW, which is consistent with the estimation in Eq. (17). Due to the finite thickness, the maxima in the case of a quantum well are shifted by a constant energy $\Delta E \sim 20$ meV. By increasing L to 60 nm, one obtains the result much closer to the bulk case [Fig. 2(c)]. In such a case, the amplitude of the oscillations is smaller in the QW due to the fact that $\text{Im}\chi \sim \frac{1}{L}$. Additionally, the increase of $\partial\chi/\partial E$ to the left of the first maximum is much weaker than for $L = 10$ nm.

The addition of the resonant term Q given by Eq. (14) into the expression for susceptibility [Eq. (13)] introduces a correction to the spectrum; due to numerical difficulties connected with the integration of functions that may potentially contain singularities, one can also change the confinement potential to derive an alternative solution in Eq. (21). Both solutions are shown in Fig. 3(a). In general, the Coulomb interaction of electron-hole pairs generates not only bound states below the gap, but also affects the continuum above the gap, with the effect of any given exciton proportional to its oscillator strength. One can see that the inclusion of excitons does not affect the period of oscillations. Both approximations predict some reduction of the oscillation amplitude (larger for modified potential) and a small overall increase of $\partial\chi/\partial E$ (roughly the same for both methods). The amplitude decreases monotonically for the case without excitons and approximation 2, while for the first approximation, there are slight local variations (most noticeable for $E = 2230$ and $E = 2280$ meV). The lack of localized oscillatory terms in the second approximation is directly linked to the fact that in the approximation in Eq. (21), there are no integrals including Airy functions. In the stronger field regime [Fig. 3(b)], both approaches are in agreement regarding the amplitude. However, one can observe a slight phase shift for the results of Eq. (13). The consistency of both approaches indicates that the underlying assumption of the second approximation, e.g., $f \rightarrow 0$, still holds for $f = 0.005$. As mentioned before, the inclusion of excitons increases the mean value of χ , especially in the high energy region (inset).

IV. CONCLUSIONS

We have examined the difference between the FK effect in the bulk and two-dimension Cu_2O structure with REs. In the theoretical description, the multiplicity of the confinement states is included by summation in the appropriate Green function over the confinement states. The calculation results indicate that the general features of the Franz-Keldysh effect

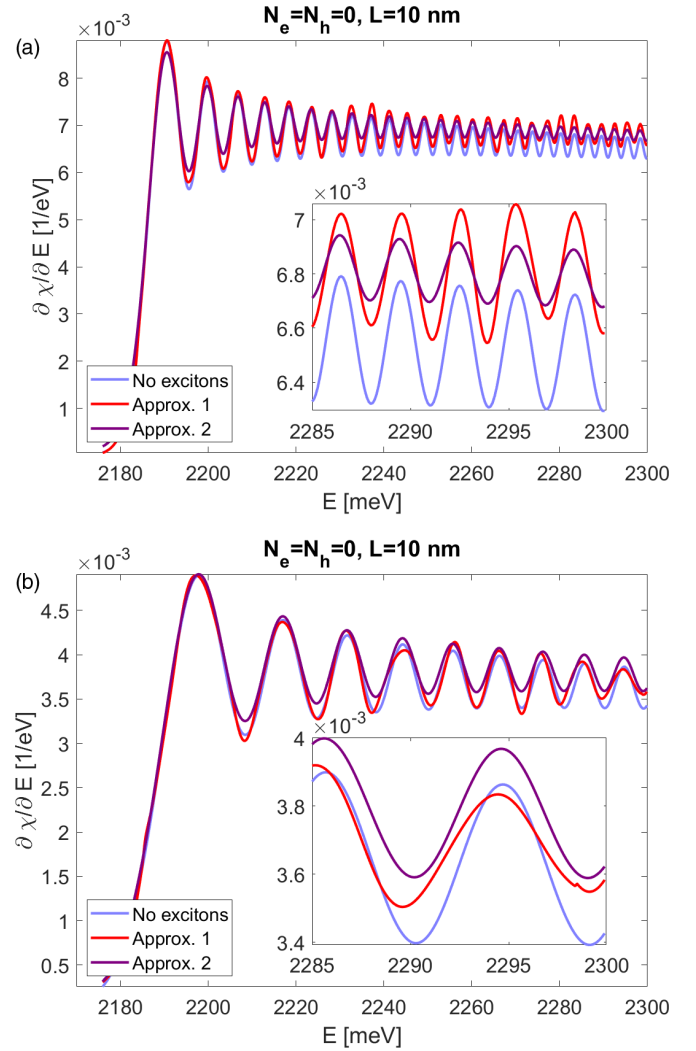


FIG. 3. Imaginary part of susceptibility in the energetic region above the band gap, calculated for (a) $f = 0.001$ and (b) $f = 0.005$, from Eq. (15) (no excitons), Eq. (13) with Eq. (14) (Approx. 1), and Eq. (21) (Approx. 2).

are preserved in the QW system. Continuous, quasiperiodic oscillations in the absorption spectrum emerge above the band gap, with a period dependent on the strength of the applied electric field. The size quantization influences the amplitudes and extrema positions of the oscillations, which in turn depend on the confinement energies. We indicate that depending on the well thickness and electric field, the oscillations connected with higher confinement states may be observable in the high energy part of the spectrum, which contrasts with the bulk case where the FK effect quickly vanishes for $E \gg E_g$. The effect consisting in a change in the absorption spectrum caused by the applied electric field is the principle of an operation of an electromodulator. By reducing the size of the system, one introduces multiple confinement states, which produce thickness-dependent interference effects in the FK spectrum. Thus, the QW system adds another degree of freedom in controlling the absorption spectrum. Finally, it is shown that the presence of excitons affects the FK spectrum in a smooth, global manner, with no localized effects such as the excitonic lines below the gap. Overall, Rydberg excitons in Cu_2O enable

convenient control and precise steering of absorption. The FK effect has not yet been observed in a Cu₂O QW, but the presented predictions confirm the tendencies of experimental observations for other semiconductors. The construction of

high-sensitivity, compact modulators based on quantum wells is the desirable goal for modern quantum engineering and we hope that the presented results will be useful for practical exploitation in the future.

-
- [1] T. Kazimierczuk, D. Fröhlich, S. Scheel, H. Stolz, and M. Bayer, *Nature (London)* **514**, 344 (2014).
- [2] M. Aßmann and M. Bayer, *Adv. Quantum Technol.* **2020**, 1900134 (2020).
- [3] M. Khazali, K. Heshami, and C. Simon, *J. Phys. B* **50**, 215301 (2017).
- [4] V. Walther, R. Johne, and T. Pohl, *Nat. Commun.* **9**, 1309 (2018).
- [5] S. Zielińska-Raczyńska, D. Ziemkiewicz, and G. Czajkowski, *Phys. Rev. B* **97**, 165205 (2018).
- [6] W. Franz, *Z. Naturforsch A* **13**, 484 (1958).
- [7] V. Keldysh, *Zh. Eksp. Teor. Fiz.* **34**, 1138 (1958) [*Sov. Phys. JETP* **7**, 788 (1958)].
- [8] A. Cavallini, L. Polenta, M. Rossi, T. Stoica, R. Calarco, R. Meijers, T. Richter, and H. Lüth, *Nano Lett.* **7**, 2166 (2007).
- [9] D. Li, J. Zhang, Q. Zhang, and Q. Xiong, *Nano Lett.* **12**, 2993 (2012).
- [10] C. Xia, S. Wei, and H. N. Spector, *Physica E* **42**, 2065 (2010).
- [11] V. Perebeinos and P. Avouris, *Nano Lett.* **7**, 609 (2007).
- [12] D. A. B. Miller, D. S. Chemla, and S. Schmitt-Rink, *Phys. Rev. B* **33**, 6976 (1986).
- [13] C. Trallero-Giner, International Atomic Energy Agency (IAEA), Report No. IC-86/282, International Nuclear Information System (INIS), Vol. 18 (1986).
- [14] D. Merbach, E. Schöll, W. Ebeling, P. Michler, and J. Gutowski, *Phys. Rev. B* **58**, 10709 (1998).
- [15] C. Xia and H. Spector, *J. Appl. Phys.* **105**, 084313 (2009).
- [16] D. Ziemkiewicz, G. Czajkowski, K. Karpiński, and S. Zielińska-Raczyńska, *Phys. Rev. B* **104**, 075303 (2021).
- [17] J. B. Dow and D. Redfield, *Phys. Rev. B* **1**, 3358 (1970).
- [18] K. Orfanakis, S. K. Rajendran, H. Ohadi, S. Zielińska-Raczyńska, G. Czajkowski, K. Karpiński, and D. Ziemkiewicz, *Phys. Rev. B* **103**, 245426 (2021).
- [19] J. Heckötter, D. Fröhlich, M. Aßmann, and M. Bayer, *Phys. Solid State* **60**, 1595 (2018).
- [20] S. Zielińska-Raczyńska, D. Ziemkiewicz, and G. Czajkowski, *Phys. Rev. B* **95**, 075204 (2017).
- [21] M. Abramowitz and I. Stegun, *Handbook of Mathematical Functions* (Dover, New York, 1965).
- [22] D. Ziemkiewicz, K. Karpiński, G. Czajkowski, and S. Zielińska-Raczyńska, *Phys. Rev. B* **101**, 205202 (2020).
- [23] D. Ziemkiewicz and S. Zielińska-Raczyńska, *Opt. Lett.* **43**, 3742 (2018).